International Journal of Innovative Computing, Information and Control
Volume **20**, Number **3**, June **2024**

ICIC International ©2024 ISSN 1349-4198
pp. **839–856**

RESEARCH ON VIBRATION SUPPRESSION OF FOUR-MASS TRANSMISSION CHAIN IN WIND POWER GENERATION SYSTEM WITH GEAR CLEARANCE

Chenyang Zhou[1], Yanxia Shen[2,*] and Yuanshen Zhou[1]

[1]School of Electronic Engineering
Jiangsu Ocean University
No. 59, Cangwu Road, Haizhou District, Lianyungang 222006, P. R. China
2022000042@jou.edu.cn; zys62@126.com

[2]School of Internet of Things Engineering
Jiangnan University
No. 1800, Lihu Avenue, Wuxi 214122, P. R. China
*Corresponding author: shenyx@jiangnan.edu.cn

Received March 2023; revised September 2023

Abstract. *The wind power system drivetrain is a multi-mass transmission system with gear clearance, and its elasticity and gear clearance cause the drivetrain to vibrate. The PID controller is used to suppress the vibration caused by the drive shaft elasticity, but not the vibration caused by the gear clearance. The internal model control (IMC) can suppress the clearance vibration, but it is only suitable for the drivetrain with fewer mass blocks. This paper aims at the vibration problem of four-mass (multi-mass) drivetrain of wind power system with gear clearance, and according to the decomposition principle of the nonlinear clearance unit, a control strategy based on disturbance observer to suppress the clearance vibration is proposed. Firstly, a four-mass drivetrain model of the wind power system with clearance is established, the cause of drivetrain clearance vibration is analyzed, and a simple method for measuring clearance vibration is proposed. Secondly, the clearance nonlinear unit is decomposed into a linear unit and a bounded disturbance unit, and a disturbance observer is used to suppress the bounded disturbance. Finally, the effect of the proposed vibration suppression scheme is verified by simulation experiments. The results show that the steady-state vibration amplitude of the drivetrain is only 0.8% after the disturbance observer suppression method is adopted, which verifies the effectiveness of the suppression scheme proposed in this paper.*

Keywords: Wind power generation system, Four-mass drivetrain, Mechanical vibration suppression, Disturbance observer, Gear clearance

1. **Introduction.** The drivetrain of doubly-fed wind power system is composed of wind turbine, gearbox, generator, and transmission shaft, etc. The vibration caused by the elasticity of transmission shaft and gear clearance mainly exists in the drivetrain. In previous research, linear control methods such as notch filter and PID controller are usually used to suppress elastic vibration [1-7]. However, the linear control method cannot suppress the nonlinear vibration of the drivetrain caused by the gear clearance.

At present, the classical control theory is used to solve the problem of nonlinear clearance vibration control, such as description function, phase plane method, and limit cycle. These methods need to draw graphs and involve nonlinear function analysis, which is difficult to work. Therefore, it is necessary to explore other methods to suppress the nonlinear vibration of gear clearance.

DOI: 10.24507/ijicic.20.03.839

According to different research purposes, the drivetrain of wind power system can be divided into different mass blocks. The more the number of mass blocks, the more it can reflect the real performance of the drivetrain. However, the more the number of mass blocks, the more complex the structure of the drivetrain, and the difficulty of mathematical model analysis and vibration suppression will increase.

In 2000, [8] proposed the theory that the nonlinear clearance property N can be expressed by the combination of a linear element H and a nonlinear bounded perturbation element d. According to this theory, in the previous work, the authors proposed the method of using internal model control to suppress the nonlinear vibration of the clearance [9,10]. When the internal model control method is used to suppress the vibration of the drivetrain, the transfer function diagram of the drivetrain needs to be transformed. This method is suitable for the system with fewer mass blocks. For systems with large number of mass blocks, the authors present a method to suppress the clearance vibration of drivetrain by using disturbance observer. This method does not need to change the structure diagram of the drivetrain, and is suitable for vibration suppression control in the four-mass drivetrain of wind power system.

The idea of disturbance observer uses a disturbance observer to observe the d of the system, and feeds back to the input to offset the disturbance factors in the system. Its working principle is very suitable for suppressing the above clearance nonlinear vibration disturbance d.

Since its establishment, the disturbance observer theory has been widely used in the practice of motor servo control [11-13]. [14] combined the proportional-differential controller (PD) with the disturbance observer (DOB) to propose a composite control algorithm to solve the vibration problem caused by mass block imbalance in magnetic bearing rotor system. In [15], a double-loop control strategy of inner loop robust control and outer loop disturbance observer was adopted to suppress the speed fluctuation on the load side in view of the vibration phenomenon generated by the actuator of industrial robots. [16] proposed an improved disturbance observer control strategy for the maximum power tracking control mode of wind power system operation. In addition, the active vibration control and disturbance observer design of floating ocean thermal energy conversion systems were researched in [17]. In [18], a vibration suppression method based on disturbance observer was proposed to solve the mechanical vibration problem of two-mass drivetrain of servo system. In [19], a PMSM vector control scheme based on torque disturbance observer was proposed, and the torque disturbance observer was designed to estimate the PMSM disturbance torque, which improves the motor control performance.

In summary, the disturbance observer method has made great progress since its birth. When applying disturbance observer method to research vibration, because it does not need to simplify the transfer function of the controlled object, it has advantages in the system with a large number of mass blocks (four masses). However, there is little literature on the application of disturbance observer with vibration suppression of multi-mass blocks in wind power system.

The organizational structure of this paper and contribution points are as follows.

1) In this section, referring to the introduction structure of [20], the research status and shortcomings of vibration suppression in the drivetrain of wind power system are introduced, and a scheme of vibration suppression with disturbance observer in the multi-mass block number drivetrain is proposed.

2) The second section describes the composition of the drivetrain of the wind power system, and establishes the model of the four-mass drivetrain including the gear clearance.

3) The third section analyzes the reasons of gear clearance causing drivetrain vibration, and puts forward a simple method to verify gear clearance vibration.

4) In the fourth section, the nonlinear clearance is decomposed into a linear link and a bounded perturbation link, and a disturbance observer method is proposed to suppress vibration in a four-mass drivetrain with clearance.

5) In the fifth section, simulation experiments verify the effectiveness of the scheme proposed for suppressing clearance vibration in this paper.

6) Finally, in the sixth section, a brief summary of the research results is given.

2. The Structure and Modeling of Four-Mass Drivetrain of Wind Power System.

2.1. **The composition of drivetrain of wind power system.** The drivetrain of the wind power system is shown in Figure 1. On the far left of the figure is a wind turbine, a planetary gear train in the gearbox by a low-speed shaft connected to it; The second stage parallel gear train of the gearbox is connected to the generator on the right side by a high-speed shaft. The gearbox is composed of three parts: planetary gear train, first stage parallel gear train and second stage parallel gear train.

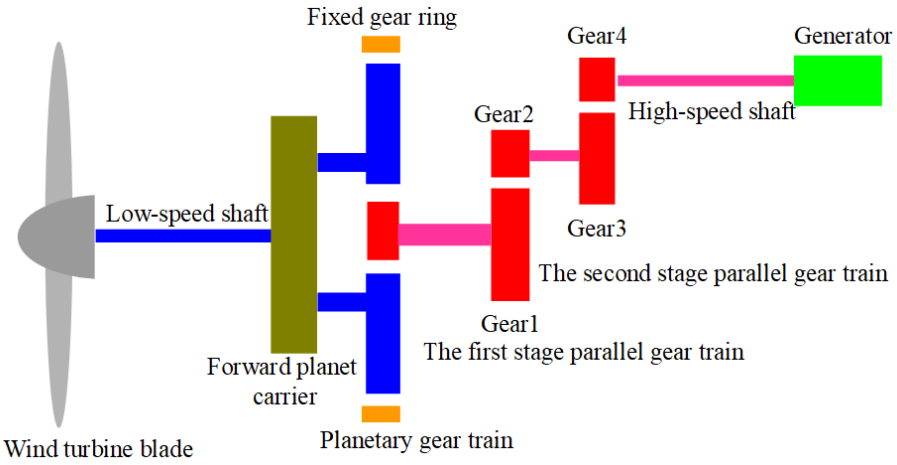

FIGURE 1. The drivetrain of wind power system with gearbox

In Figure 1, the gearbox is divided into three components: the planetary gear train, the first stage parallel gear train, and the second stage parallel gear train. A low-speed shaft connects the gearbox's planetary gear train to the wind turbine, while a high-speed shaft connects the gearbox's second parallel gear train to the generator on the right. The gearbox's three gears are equivalent to a pair of gears. In Figure 1, the equivalent gear's driving gear comprises the planetary frame and planetary gear train. In contrast, the driven gear comprises the sun wheel, the first-level parallel gear train, and the second-level parallel gear train. The gear clearance is the equivalent sum of the three gear train. Figure 2 illustrates the equivalent gear's motion relation schematically. The driving gear J_{C1} drives the driven gear J_{C2} through a clearance delay of $2b$. The four-mass drivetrain of wind power system with gear clearance comprises four-mass blocks of the wind turbine, wind turbine side gear J_{C1}, generator side gear J_{C2} and generator, and connecting shaft and gear clearance.

2.2. **The structure and modeling of four-mass drivetrain of wind power system without gear clearance.**

1) The structure of the four-mass drivetrain without gear clearance

The four-mass drivetrain of the wind power system without clearance can be represented by the model shown in Figure 3.

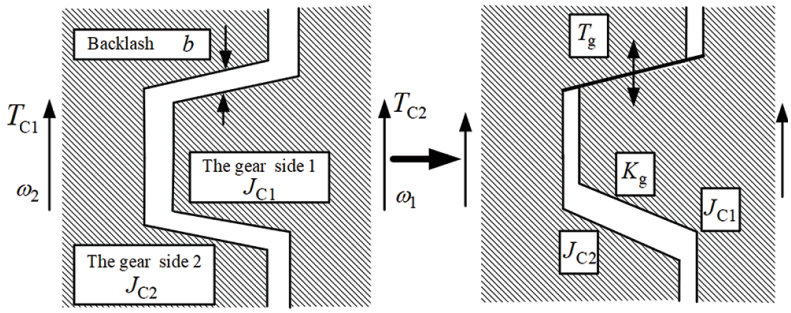

FIGURE 2. The schematic diagram of gear structure and motion relation

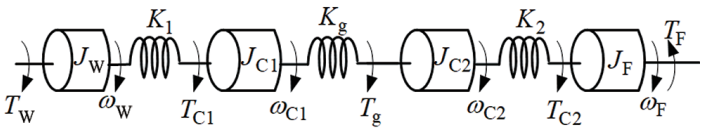

FIGURE 3. The schematic diagram of four-mass drivetrain

In Figure 3, T_{W}, T_{C1}, T_{g}, T_{C2} and T_{F} denote the driving torque of the wind turbine, gearbox driving gear torque, gear transmission torque, driven gear torque, and the resistance torque of the generator, respectively. ω_{W}, ω_{C1}, ω_{C2}, and ω_{F} represent the speed of wind turbine rotation, driving gear, driven gear, and generator, respectively; J_{W}, J_{C1}, J_{C2}, and J_{F} denote the rotational inertia of the wind turbine mass block, driving gear, driven gear, and generator mass block, respectively. K_1 is the low-speed shaft elasticity coefficient of the gearbox connected to the wind turbine. K_{g} is the gear transmission elasticity coefficient, K_2 is the high-speed shaft elasticity coefficient of the gearbox connected to the generator.

2) Modeling of four-mass drivetrain

In Figure 3, wind turbine, driving gear C1, driven gear C2 and generator are taken as research objects. Because the drivetrain's vibration is discussed in this paper, the gear ratio is assumed to be one for simplicity when deriving the transfer function of the four-mass drivetrain.

When modeling the drivetrain, the gear clearance link is not considered. According to Figure 3, it can be obtained as follows.

The motion equation of wind turbine is

$$T_{\mathrm{W}} - T_{\mathrm{C1}} = J_{\mathrm{W}} \frac{\mathrm{d}\omega_{\mathrm{W}}}{\mathrm{d}t} \tag{1}$$

The torque equation of low speed elastic shaft is

$$T_{\mathrm{C1}} = K_1 \int (\omega_{\mathrm{W}} - \omega_{\mathrm{C1}}) \mathrm{d}t \tag{2}$$

The motion equation of the mass block of the driving gear is

$$T_{\mathrm{C1}} - T_{\mathrm{g}} = J_{\mathrm{C1}} \frac{\mathrm{d}\omega_{\mathrm{C1}}}{\mathrm{d}t} \tag{3}$$

The torque equation of gear transmission is

$$T_{\mathrm{g}} = K_{\mathrm{g}} \int (\omega_{\mathrm{C1}} - \omega_{\mathrm{C2}}) \mathrm{d}t \tag{4}$$

The motion equation of the mass block of the driven gear is

$$T_{\mathrm{g}} - T_{\mathrm{C2}} = J_{\mathrm{C2}} \frac{\mathrm{d}\omega_{\mathrm{C2}}}{\mathrm{d}t} \tag{5}$$

The torque equation of high speed elastic shaft is

$$T_{\mathrm{C2}} = K_2 \int (\omega_{\mathrm{C2}} - \omega_{\mathrm{F}}) \mathrm{d}t \tag{6}$$

The motion equation of the generator is

$$T_{\mathrm{C2}} - T_{\mathrm{F}} = J_{\mathrm{F}} \frac{\mathrm{d}\omega_{\mathrm{F}}}{\mathrm{d}t} \tag{7}$$

Setting $T_{\mathrm{F}} = 0$, the Laplace transform of Equations (1) to (7) is obtained

$$\begin{cases} J_{\mathrm{W}}\omega_{\mathrm{W}} \cdot s = T_{\mathrm{W}} - T_{\mathrm{C1}} & (8) \\ T_{\mathrm{C1}} = \dfrac{K_1}{s}(\omega_{\mathrm{W}} - \omega_{\mathrm{C1}}) & (9) \\ J_{\mathrm{C1}}\omega_{\mathrm{C1}} \cdot s = T_{\mathrm{C1}} - T_{\mathrm{g}} & (10) \\ T_{\mathrm{g}} = \dfrac{K_{\mathrm{g}}}{s}(\omega_{\mathrm{C1}} - \omega_{\mathrm{C2}}) & (11) \\ J_{\mathrm{C2}}\omega_{\mathrm{C2}} \cdot s = T_{\mathrm{g}} - T_{\mathrm{C2}} & (12) \\ T_{\mathrm{C2}} = \dfrac{K_2}{s}(\omega_{\mathrm{C2}} - \omega_{\mathrm{F}}) & (13) \\ J_{\mathrm{F}}\omega_{\mathrm{F}} \cdot s = T_{\mathrm{C2}} & (14) \end{cases}$$

According to Equations (8)-(14), the transfer function structure diagram of the four-mass block drivetrain without clearance can be obtained, as shown in Figure 4.

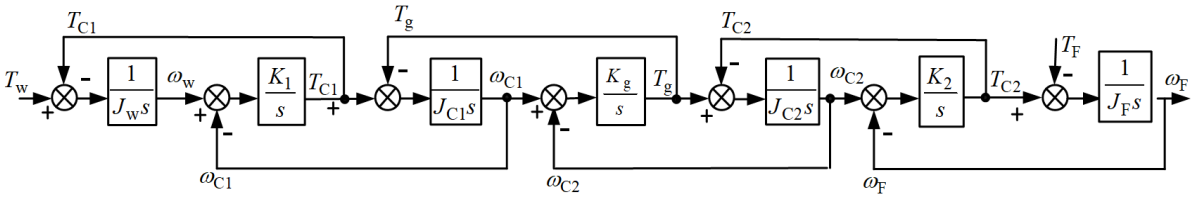

FIGURE 4. The transfer function structure diagram of four-mass drivetrain without clearance

2.3. **Modeling of four-mass drivetrain of wind power system with gear clearance.**

1) Nonlinear characteristic of gear clearance

The nonlinear characteristic of gear clearance is shown in Figure 5.

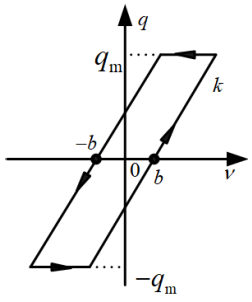

FIGURE 5. The nonlinear characteristic with gear clearance

The input-output relationship of gear clearance can be obtained from Figure 5 as follows

$$q = \begin{cases} k(v-b); & \dfrac{\mathrm{d}q}{\mathrm{d}t} > 0 \\ k(v+b); & \dfrac{\mathrm{d}q}{\mathrm{d}t} < 0 \\ q_{\mathrm{m}} sgn(v); & \dfrac{\mathrm{d}q}{\mathrm{d}t} = 0 \end{cases} \tag{15}$$

In Equation (15), the input is the position v of the driving gear, the output is the position q of the driven gear, $2b$ is the total clearance in the drivetrain, and the characteristic slope is k.

2) Modeling of drivetrain of wind power system with gear clearance

In this paper, a nonlinear clearance module N is proposed to represent the equivalent total clearance of three gear trains in the gearbox, and then the nonlinear clearance module N is added to the transfer function structure diagram shown in Figure 4, thus obtaining the transfer function structure diagram of the drivetrain with gear clearance, as shown in Figure 6.

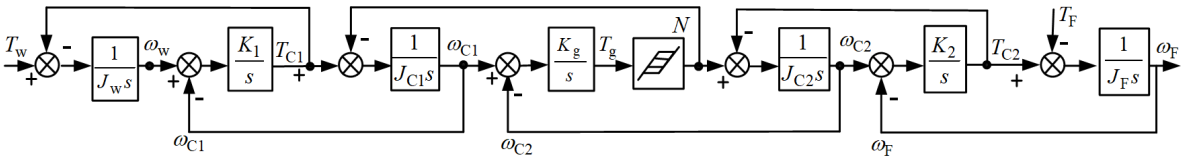

FIGURE 6. The transfer function structure diagram of four-mass drivetrain with clearance

3. **Vibration Analysis of Drivetrain of Wind Power System with Gear Clearance.** Gear clearance has two primary effects on the control system.

1) Decrease the output signal amplitude and introduce phase lag. As shown in Figure 7, the output signal is limited by the effect of q_{m} on gear clearance characteristic. As a

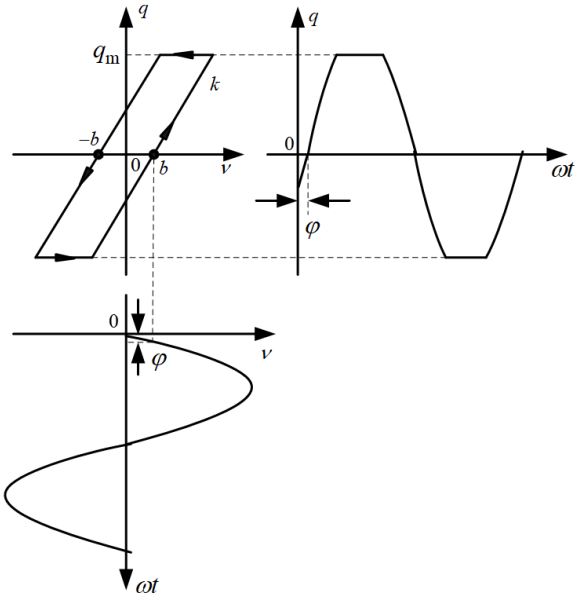

FIGURE 7. The influence on output signals with clearance

result of gear clearance $2b$, the output signal lags behind the input signal in phase by an angle of φ. Thus, the stability and dynamic performance of the system are affected, and the system's instability is increased.

2) When there is nonlinearity in the gear clearance, the four-mass drivetrain transitions from the linear system depicted in Figure 4 to the nonlinear system.

The gear clearance vibration can be verified by the following simple method: The transfer functions of the four-mass drivetrain depicted in Figure 6 were used to create a wind turbine speed closed-loop control system. The system's output with clearance is subtracted from the system's output without clearance to obtain the difference between the two outputs, which represents the nonlinear unit's influence result with clearance. The verification scheme is shown in Figure 8, the output waveform is shown in Figure 9, and the drivetrain parameters are shown in Table 1, in Section 5.1.

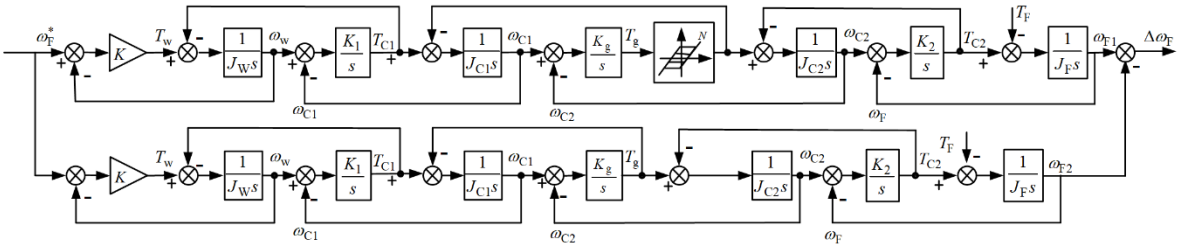

FIGURE 8. The experimental scheme of nonlinear vibration of clearance

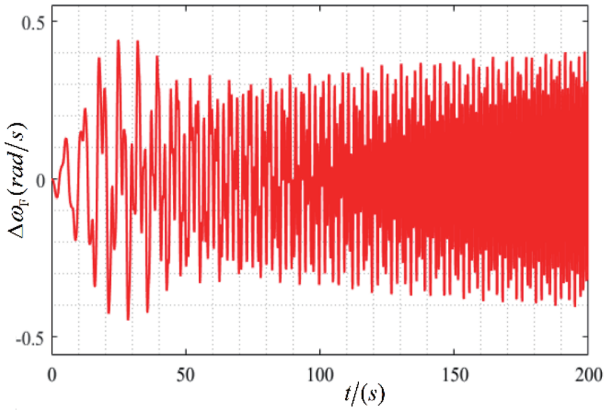

FIGURE 9. The generator speed deviation vibration waveform caused by clearance

As illustrated in Figure 9, the nonlinearity of the gear clearance results in system output vibration.

4. Gear Clearance Vibration Suppression Strategy Based on Disturbance Observer.

4.1. Equivalence of nonlinear characteristic of gear clearance. In Figure 10, the role of nonlinear gear clearance N in the system can be represented by the equivalent unit in the dotted box, where N is decomposed into two parts, $N = H + d$ [8]. $H(s)$ is a linear time-invariant system, and $d(s)$ is a nonlinear time-varying system, representing a bounded disturbance. When the nonlinearity of gear clearance is expressed as the bounded disturbance $d(s)$, the disturbance observer can be used to estimate the nonlinear factor $d(s)$ of gear clearance and feedback to the input end to offset the nonlinear influence in the system, resulting in N exhibiting linear performance.

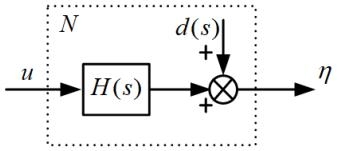

FIGURE 10. The nonlinear model of gear clearance

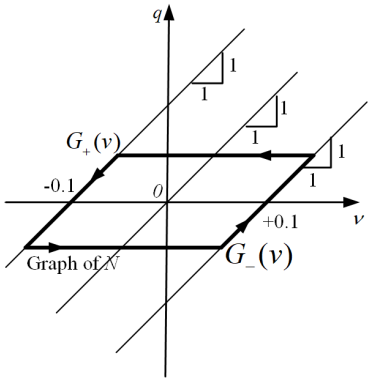

FIGURE 11. The equivalence of clearance characteristic

The clearance characteristics N of the drivetrain of the wind power system are shown in Figure 11.

Obviously, for all v, the graph of N lies between or on two parallel lines $G_+(v) = kv + b$ and $G_-(v) = kv - b$. Thus, N can be decomposed into $N = H + d$, where the transfer function of the linear part is $H(s) = k$, that is, the straight line passing through the origin of coordinates in the figure. $d(s)$ is a nonlinear disturbance function bounded by b, in this case, $2b = 0.2$. For the sake of convenience of transformation, the slope k of the clearance characteristic is set to one. Then, the nonlinear unit N can be represented by $H(s) = 1$ and the nonlinear bounded disturbance function $d(s)$ in the dotted box in Figure 10.

4.2. **Principle of suppressing gear clearance vibration by disturbance observer.** This paper presents a method to suppress the nonlinear vibration of gear clearance with disturbance observer. This method is also based on the principle that the nonlinear N of gear clearance can be represented by a combination of a linear time-invariant system $H(s)$ and a nonlinear time-varying system $d(s)$. When the nonlinear factor associated with gear clearance is expressed as a nonlinear bounded disturbance $d(s)$, the disturbance observer method can be used to suppress the vibration caused by gear clearance in the multi-mass drivetrain.

Figure 12 illustrates the fundamental disturbance observer principle in block diagram form. It equates the deviation between the actual and model outputs caused by the external disturbance $d(s)$ and the model parameter change as the system's input; the equivalent disturbance is observed. Then, by introducing equal compensation at the input, the disturbance is completely suppressed.

The use of disturbance observer to suppress the clearance vibration of wind power system drivetrain does not need to transform the structure diagram of the controlled object, as long as the original structure of the controlled object is preserved. This is very important for vibration suppression control of multi-mass drivetrain.

In Figure 12, $G_2(s)$ denotes the transfer function of the controlled object and $G_2^{-1}(s)$ is the inverse of the controlled object, $d(s)$ is the external disturbance, $\hat{d}(s)$ is the observation value of equivalent disturbance, and $U(s)$ is the control input. The observed value of

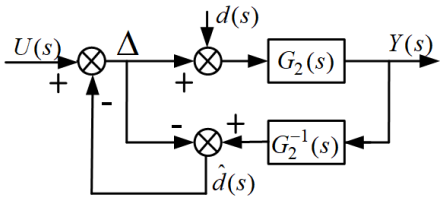

FIGURE 12. The basic disturbance observer schematic diagram

equivalent disturbance $\hat{d}(s)$ can be obtained from Figure 12.

$$\hat{d}(s) = [\Delta - d(s)]G_2(s)G_2^{-1}(s) - \Delta = -d(s) \tag{16}$$

Equation (16) demonstrates that the accurate estimation of disturbance can be realized through disturbance observation value. The disturbance observer in Figure 12 still has problems in practical application. The solution is to insert a low-pass filter $Q(s)$ behind $\hat{d}(s)$ and replace $G_2^{-1}(s)$ with the inverse $D_2(s)$ of the ideal model. The block diagram depicted in Figure 13 is obtained.

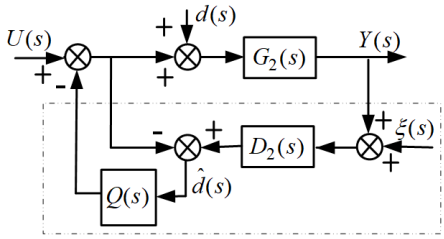

FIGURE 13. The transfer function structure diagram of the disturbance observer

The low-frequency disturbance can be effectively compensated for using the low pass filter $Q(s)$, and the high-frequency noise can be effectively filtered using the high pass filter $Q(s)$. The feedback control system depicted in Figure 14 is based on a disturbance observer and can be used to suppress nonlinear gear clearance.

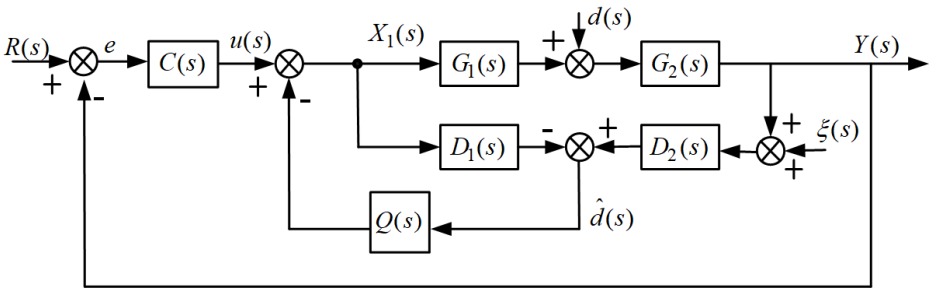

FIGURE 14. The feedback control system with disturbance observer

In order to make the disturbance observer physically realizable and reduce the impact of high frequency measurement noise, $Q(s)$ filters are usually connected in series at the output end of the disturbance observer, and the relative order of the filter is required to be equal to or higher than that of the actual model.

4.3. **Gear clearance vibration suppression system based on disturbance observer.** According to the analysis of the above disturbance observer principle, when the nonlinear factor of gear clearance in the drivetrain of wind power system is expressed as

nonlinear bounded disturbance $d(s)$, the disturbance observer method can be used to suppress the vibration caused by gear clearance. Figure 14 shows the feedback control system based on disturbance observer, which can be used to suppress the nonlinear influence of gear clearance in the drivetrain of wind power system.

The transfer function of each unit in Figure 14 is as follows.

1) $C(s)$ is the PID controller used by the system to suppress elastic vibration, and the parameters are shown in Section 5.1.

2) $G_2(s)$ is the integral unit of rotational inertia of the wind turbine:

$$G_2(s) = \frac{1}{J_{\mathrm{W}} s}$$

3) $G_1(s)$ corresponds to the linear time-invariant system $H(s)$ in the nonlinear unit N. In this case, $H(s) = 1$.

4) $D_1(s)$ and $D_2(s)$ are nominal models corresponding to $G_1(s)$ and $G_2(s)$, respectively. $d(s)$ represents the nonlinear factor (bounded disturbance) of gear clearance, which is moved to $G_2(s)$ before by structural diagram transformation. When the disturbance observation value accurately reflects the disturbance, the following occurs:

$$D_1(s) = H(s) = 1; \quad D_2(s) = 1/G_2(s) = J_{\mathrm{W}} s$$

The following analysis can be performed using the structural relationship depicted in Figure 14.

1) The disturbance observation value accurately reflects the disturbance condition

In Figure 14, without considering the high-frequency noise $\xi(s)$, the observed disturbance value is

$$\hat{d}(s) = [D_2(s) \cdot G_1(s) \cdot G_2(s) - D_1(s)] X_1(s) + D_2(s) \cdot G_2(s) \cdot d(s) \tag{17}$$

The conditions that make this equation $\hat{d}(s) = d(s)$ are true:

$$\begin{cases} D_2(s) \cdot G_1(s) \cdot G_2(s) = D_1(s) \\ D_2(s) \cdot G_2(s) = 1 \end{cases} \text{ that is, } \begin{cases} D_1(s) = G_1(s) \\ D_2(s) = 1/G_2(s) \end{cases} \tag{18}$$

2) The condition that the disturbance does not affect the system output

The output Y(s) of Figure 14 is

$$Y(s) = \frac{G_1(s) \cdot G_2(s) \cdot C(s) \cdot R(s) + G_2(s) \cdot d(s)[1 - Q(s) \cdot G_1(s)]}{1 + G_1(s) \cdot G_2(s) \cdot C(s)} \tag{19}$$

When $\hat{d}$ and d are fully compensated, that is, when the influence of d is not included in the output Y, the following conditions must be satisfied:

$$1 - Q(s) \cdot G_1(s) = 0, \text{ that is, } Q(s) = 1/G_1(s) \tag{20}$$

3) Design of filter $Q(s)$

The three factors that need to be considered in designing a low-pass filter $Q(s)$, are the time constant, the order of the numerator and the order of the denominator. The form of a first-order low-pass filter commonly used is

$$Q(s) = \frac{\lambda_1}{s + \lambda_2} = \frac{\lambda_1/\lambda_2}{Ts + 1} \tag{21}$$

where $T = 1/\lambda_2$, λ_1 and λ_2 are constants.

When the three parameters of the disturbance observer are selected, their relation to each other is

a) The smaller the time constant of $Q(s)$, the higher the corresponding transition frequency, and the wider the frequency band. Generally, the time constant of $Q(s)$ is much smaller than the time constant of the system.

b) The smaller the time constant of $Q(s)$, the more sensitive the system is to high-frequency noise. The greater the difference between the numerator and denominator order, the stronger the ability to restrain high-frequency noise.

4) The influence of low-pass filter $Q(s)$ on the disturbance observer performance

In the disturbance observer, $Q(s)$ has a significant effect on the disturbance observer's performance. In Figure 14, the transfer functions of output $Y(s)$ to input $U(s)$, disturbance $d(s)$, and high-frequency noise $\xi(s)$ are shown in Equations (22), (23), and (24), respectively. Assuming the other two inputs are zero, the transfer function of output to input is as follows:

$$W_{Y/U}(s) = \frac{G_1(s) \cdot G_2(s)}{1 + Q(s) \cdot G_1(s) \cdot G_2(s) D_2(s) - Q(s) \cdot D_1(s)} \tag{22}$$

$$W_{Y/d}(s) = \frac{G_2(s)[1 - Q(s) \cdot D_1(s)]}{1 + Q(s) \cdot G_1(s) \cdot G_2(s) D_2(s) - Q(s) D_1(s)} \tag{23}$$

$$W_{Y/\xi}(s) = \frac{-Q(s) \cdot G_1(s) \cdot G_2(s) \cdot D_2(s)}{1 + Q(s) \cdot G_1(s) \cdot G_2(s) \cdot D_2(s) - Q(s) \cdot D_1(s)} \tag{24}$$

The design principle of $Q(s)$ is as follows: in the low-frequency band, $Q(s) = 1$; in the high-frequency band, $Q(s) = 0$.

1) In the low-frequency band, $Q(s) = 1$

According to Equation (22):

$$W_{UY}(s) = G_1(s) G_2(s) \tag{25}$$

a) Equation (25) demonstrates that a disturbance observer can effectively compensate for low-frequency interference in the low-frequency band, ensuring that the actual object's response is consistent with the nominal model's, thereby ensuring good robustness.

According to Equation (23) and Equation (20),

$$W_{dY}(s) = 0 \tag{26}$$

b) According to Equation (26), the disturbance observer is capable of completely suppressing low-frequency interference in the $Q(s)$ frequency band.

According to Equation (24) and Equation (20),

$$W_{\xi Y}(s) = -1 \tag{27}$$

c) Equation (27) demonstrates how low-frequency measurement noise significantly affects the disturbance observer. As a result, low-frequency noise in state measurement must be reduced in practice.

2) In the high-frequency band, $Q(s) = 0$.

According to Equation (22):

$$W_{Y/U}(s) = G_1(s) G_2(s) \tag{28}$$

According to Equations (21) and (23),

$$W_{Y/d}(s) = G_2(s) \tag{29}$$

According to Equations (22) and (24),

$$W_{Y/\xi}(s) = 0 \tag{30}$$

In high-frequency band, $W_{Y/\xi}(s) = 0$. As can be seen, the disturbance observer is insensitive to measurement noise and is capable of filtering out high-frequency noise effectively. Nonetheless, it has no inhibitory effect on object parameter perturbation or external disturbances.

Therefore, a low-pass filter $Q(s)$ is required to effectively compensate for low-frequency interference and effective high-frequency noise filtering. This system employs the simplest first-order low pass filter possible, and the filter form is shown as Equation (21).

From the above analysis, we can see

Whether in the low frequency or in the high band, the low-pass filter $Q(s)$ can realize the effective tracking of the output to the input, as shown in Equation (25) and Equation (28).

The low pass filter $Q(s)$ can be used to effectively compensate the low frequency disturbance. As shown in Equation (26).

The low-pass filter $Q(s)$ can effectively filter out high-frequency noise, as shown in Equation (30).

5. **Simulation Experiment and Result Analysis.**

5.1. **The vibration suppression experiments based on PID controller without clearance.**

1) Simulation experiment scheme

The experimental scheme is shown in Figure 15(a). The PID controller with soft start function is in the dotted box. The parameters of the drivetrain [21] in the figure are shown in Table 1; After PSO optimization, the PID controller parameters are $K_{\mathrm{p}} = 3.14$, $K_{\mathrm{i}} = 0.8$, $K_{\mathrm{d}} = 0.31$.

Table 1. The simulation experiment parameters

Number	Parameter	Value
1	J_{W} (kg.m^2)	2.44
2	J_{C1} (kg.m^2)	0.16
3	J_{C2} (kg.m^2)	0.272
4	J_{F} (kg.m^2)	0.505
5	K_1 (N.m/rad)	3.51
6	K_{g} (N.m/rad)	0.9
7	K_2 (N.m/rad)	0.516
8	$2b$ (rad)	0.2

2) Simulation experiment results and analysis

In Figure 15(b), ω_{W} is the wind turbine speed waveform, and ω_{W}^* is the wind turbine speed input reference waveform; In Figure 15(c), ω_{F} is the generator speed waveform, and ω_{F}^* is the generator speed input reference waveform.

The experimental results show that when the drivetrain does not contain the clearance, the soft start PID controller can eliminate the vibration after parameter optimization by PSO algorithm. Because the generator adopts speed open loop control, its speed control performance is worse than that of wind turbine.

5.2. **The vibration suppression experiments based on PID controller with clearance.**

1) Simulation experiment scheme

The experimental scheme is shown in Figure 16(a). A clearance nonlinear unit N is inserted into the gearbox of the four-mass drivetrain, and other conditions are the same as Section 5.1.

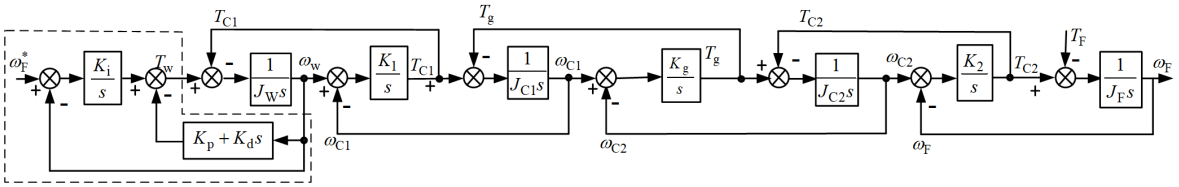

(a) The experimental scheme without clearance

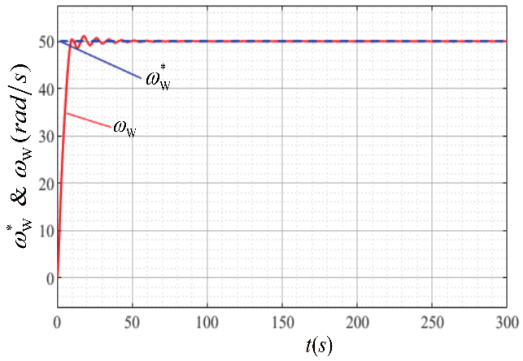

(b) The wind turbine speed waveform

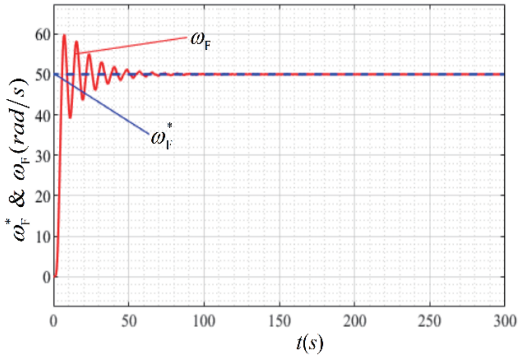

(c) The generator speed waveform

FIGURE 15. The experimental scheme and speed waveforms of four-mass drivetrain vibration suppression without clearance based on PID controller

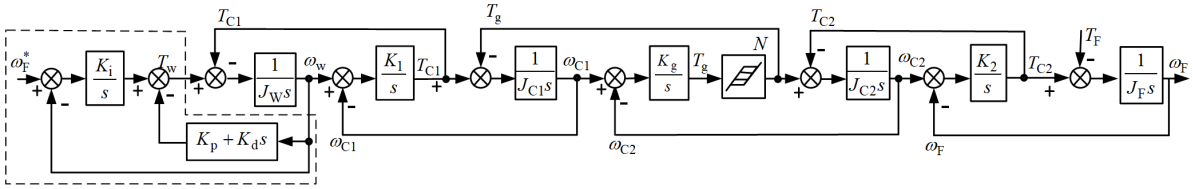

(a) The experimental scheme with clearance

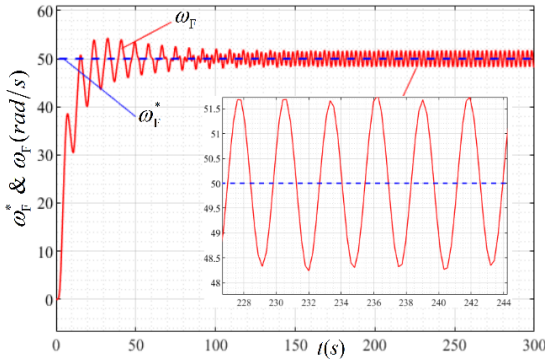

(b) The generator speed waveform

FIGURE 16. The experimental scheme and speed waveform of four-mass drivetrain vibration suppression with clearance based on PID controller

2) Simulation experiment results and analysis

Figure 16(b) shows the output speed waveform of the generator. As can be seen from the figure, the output speed of the generator vibrates. In Figure 16(b), ω_F is the generator speed waveform, and ω_F^* is the generator speed input reference waveform.

The simulation results show that when the drivetrain contains a gear clearance, the PID controller used in Section 5.1 cannot eliminate the vibration generated by the clearance, and the output speed waveform of the generator vibrates.

5.3. **The vibration suppression experiments based on disturbance observer with clearance.**

1) Simulation experiment scheme

The experimental scheme of vibration suppression based on disturbance observer proposed in this paper is shown in Figure 17(a). The disturbance observer feedback control system shown in Figure 14 is used to control the drivetrain of wind power system with clearance unit. Compared with the experimental scheme in Figure 16(a), the disturbance observer component is added. The parameters in the drivetrain are the same as those in Figure 16(a), and the structure and parameters of controller $C(s)$ are also the same as those in the dotted box in Figure 16(a). The form and parameters of the filter $Q(s)$ are as follows:

$$Q(s) = \frac{\lambda_1}{s+\lambda_2} = \frac{\lambda_1/\lambda_2}{Ts+1} = \frac{3.14}{0.4s+1}$$

2) Simulation experiment results and analysis

In Figure 17(b), ω_{F} is the generator speed waveform, and ω_{F}^* is the generator speed input reference waveform. The generator speed waveform shows that there is almost no vibration in the speed of the generator.

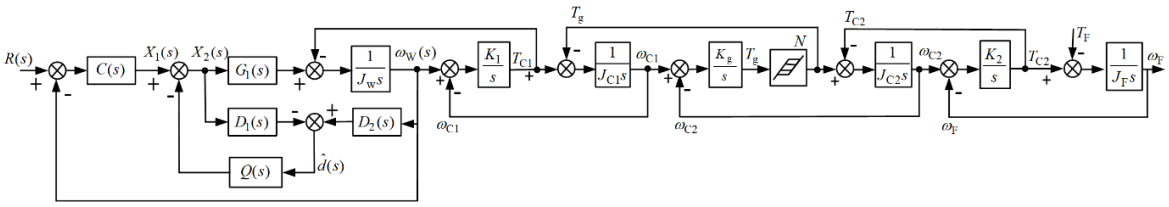

(a) The experimental scheme

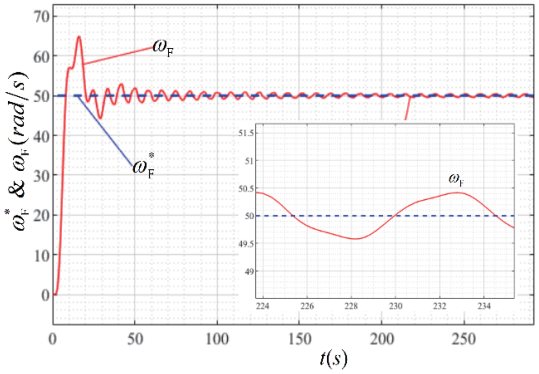

(b) The generator speed waveform

FIGURE 17. The experimental scheme and speed waveform of four-mass drivetrain vibration suppression with clearance based on disturbance observer

5.4. **The vibration suppression experiments based on shaft torque compensator with clearance.**

1) Simulation experiment scheme

[22] shows the experimental scheme of vibration suppression based on shaft torque compensator, the drivetrain is replaced with four-mass blocks. The parameters of the

drivetrain, the structure and parameters of the controller $C(s)$ are the same as those in Figure 16(a).

2) Simulation experiment results and analysis

Figure 18 shows the generator output speed waveform, in the figure, ω_{F} is the generator speed waveform, ω_{F}^{*} is the generator speed input reference waveform. It can be seen from Figure 18 that there is a large vibration in the generator speed.

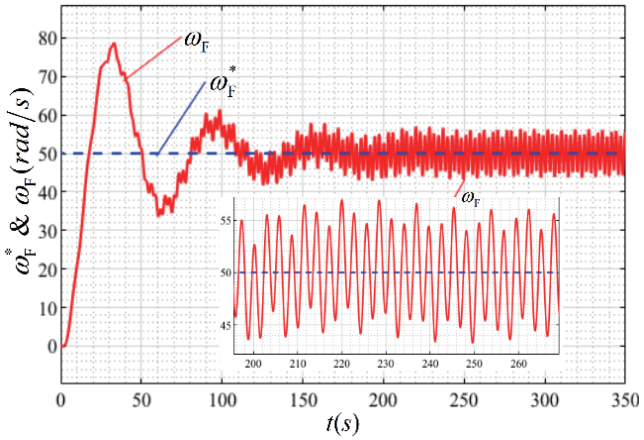

FIGURE 18. The speed waveform of four-mass drivetrain vibration suppression with clearance based on shaft torque compensator

5.5. **The vibration suppression ability comparison of the different control algorithms.** The generator speed waveforms in Figure 16(b), Figure 17(b) and Figure 18 are compared from the following three aspects.

1) The comparison of starting overshoot $\sigma\%$

From the waveforms and the data in the second column of Table 2, we can see a) the maximum overshoot of PID controller method is 8%, and its value is the smallest among the three algorithms, and several wave heads reach or approach the maximum overshoot; b) the maximum overshoot of the disturbance observer method is 30%, the maximum overshoot has only one wave head, and the rest waveforms decay quickly; c) the maximum overshoot of the shaft torque compensator method is 56%, the value is the largest among the three algorithms, and the waveform attenuation is slow.

TABLE 2. The vibration suppression ability comparison of the different control algorithms

Control algorithm	Starting overshoot $\sigma\%$	Response time t_s	Steady-state vibration amplitude $\Delta\%$
PID controller	8%	120	3.2%
Disturbance observer	30%	75	0.8%
Shaft torque compensator	56%	200	12%

2) The comparison of adjustment time t_s

From the waveforms and the data in the third column of Table 2, we can see a) the adjustment time of the disturbance observer method is about 75 seconds, which is the shortest; b) PID controller method is about 120 seconds; c) shaft torque compensator method is about 200 seconds, the longest adjustment time.

3) The comparison of steady-state vibration amplitude $\Delta\%$

Steady-state vibration amplitude is the vibration amplitude of the drivetrain for long-term stable operation, and this amplitude has the greatest influence on the drivetrain. From the close-up waveforms and the fourth column data in Table 2, it can be seen that a) the steady-state vibration amplitude of the disturbance observer method is 0.8%, which is the smallest; b) PID controller method is 3.2%; c) the shaft torque compensator method is 12%, which is the largest among the three algorithms.

By comparing the overshoot, adjustment time and steady-state vibration amplitude of PID controller, disturbance observer and shaft torque compensator method, the comprehensive performance of the disturbance observer control algorithm proposed in this paper is optimal.

6. **Conclusion.** In this paper, vibration and suppression of four-mass drivetrain of wind power system are researched, and the influence of gear clearance on drivetrain vibration is considered. The following work is done.

1) The mass blocks of the wind power system drivetrain are newly divided, and the structure of the four-mass block drivetrain is proposed, so as to analyze the performance of the wind power system drivetrain more accurately.

2) The four-mass drivetrain model of wind power system with clearance is established. Firstly, the four-mass block drivetrain model without clearance is established, and then the clearance nonlinear module is added to obtain the four-mass block drivetrain model with clearance.

3) A simple experiment scheme for verifying the clearance vibration is proposed, and it is proved that the gear clearance in the drivetrain will cause the drivetrain vibration.

4) According to the equivalent decomposition principle of the clearance nonlinear characteristics, the clearance nonlinearing is equivalent to the bounded disturbance of the linear system, and the disturbance observer is used to suppress the gear clearance vibration.

5) Simulation experiments verify that PID controller based on PSO can eliminate elastic vibration of drivetrain without clearance, but cannot eliminate clearance vibration. The vibration suppression method of disturbance observer can solve the multi-mass drivetrain vibration with clearance, and it does not need to change the structure relationship of the drivetrain.

REFERENCES

[1] C. Su, X. Wang, Z. Xu et al., Research on elastic vibration suppression of missile attitude control system, *Journal of Projectiles, Rockets, Missiles and Guidance*, vol.39, no.5, pp.154-157, 2019.

[2] J. Ma, Y. Zhang, G. Li et al., Study on vibration suppression technology of permanent magnet synchronous motor based on particle swarm optimization algorithm to optimize trap parameters, *Micromotors*, vol.53, no.11, pp.113-119, 2020.

[3] S. Bai, C. Wei, Y. Chen et al., Fuzzy PID active suppression of torsional vibration of range extenders for three-cylinder engines, *Noise and Vibration Control*, vol.42, no.2, pp.51-58, 2022.

[4] Y. He and Z. He, Vibration suppression of servo direct drive shaft in wafer level flip-chip equipment, *Machine Tool & Hydraulics*, vol.48, no.14, pp.1-5, 2020.

[5] T. Zhang, B. Qin and X. Liu, Vibration analysis and suppression of robot joints based on flexible dynamics model, *Journal of Vibration, Measurement & Diagnosis*, vol.53, no.11, pp.113-119, 2020.

[6] W. Ding, W. He, H. Chen et al., Dynamic characteristics and vibration suppression of milling and grinding robot, *Machinery Design & Manufacture*, vol.381, no.11, pp.102-105, 2022.

[7] Y. Kang, H. Shen and X. Luo, Fast suppression of mechanical resonance based on SDFT and adapting three parameters notch filter, *Micromotors*, vol.51, no.5, pp.25-30, 2018.

[8] S. M. Shahruz, Performance enhancement of a class of nonlinear systems by disturbance observers, *IEEE/ASME Transactions on Mechatronics*, vol.5, no.3, pp.319-323, 2000.

[9] C. Zhou, Y. Shen and Z. Wang, Research on vibration suppression of drivetrain in wind power generation system with gear clearance based on internal model control, *International Journal of Innovative Computing, Information and Control*, vol.18, no.4, pp.1247-1263, 2022.
[10] C. Zhou and Y. Shen, A 2-DOF-IMC method for suppressing drivetrain vibration of wind power generation system with a clearance, *Advances in Mechanical Engineering*, vol.53, no.10, pp.1-13, 2022.
[11] H. Ji, S. Wang, S.-R. Huang et al., Anti-disturbance study of servo system based on disturbance observer, *Small & Special Electrical Machines*, vol.45, no.4, pp.57-61, 2017.
[12] Y. Wang, B. Wu and T. Zhou, Vibration suppression for the space manipulator flexible joint based on disturbance observer, *Automation & Instrumentation*, vol.233, no.3, pp.147-150, 2019.
[13] W. Li, Y. Liu, S. Ge et al., Research of mechanical resonance analysis and suppression control method of the servo drive system, *Shock and Vibration*, DOI: 10.1155/2021/5627734, 2021.
[14] Z. Yue, H. Ouyang, G. Zhuang et al., Vibration suppression of rotor system of magnetic bearing based on disturbance observer, *Computer Simulation*, vol.37, no.11, pp.255-259, 2020.
[15] B. Luo, Z. Wu and M. Zhan, Research of robust disturbance observer double-loop compensation control for joint vibration of industrial robotics, *Mechanical Science and Technology for Aerospace Engineering*, vol.41, no.4, pp.530-536, 2022.
[16] H. Shi, K. Zhang and T. Guo, Maximum power control of wind power generation system based on disturbance observer, *Proceedings of the CSU-EPSA*, vol.31, no.7, pp.135-142, 2019.
[17] X. He, X. Wang, Z. Zhao et al., Disturbance rejection and vibration control for a floating ocean thermal energy conversion system, *Acta Automatica Sinica*, vol.45, no.1, pp.1846-1856, 2019.
[18] S. Wang, D. Li and X. Ren, Low frequency active resonance suppression based on unknown dynamics estimator for dual inertia servo systems, *Control Theory & Applications*, vol.37, no.12, pp.2535-2542, 2020.
[19] X. Liu, Vector control of marine permanent magnet synchronous motor based on torque disturbance observer and repetitive control, *Motor and Control Application*, vol.47, no.5, pp.33-38, 2020.
[20] K. Eguchi, D. Nakashima, T. Ishibashi and Y. Kino, Simulation and analysis of a multiple-input single-output AC/DC converter for 13.56 MHz wireless power transfer systems, *International Journal of Innovative Computing, Information and Control*, vol.18, no.3, pp.989-997, 2022.
[21] Z. Xu and Z. Pan, Influence of different flexible drivetrain models on the transient responses of DFIG wind turbine, *2011 International Conference on Electrical Machines and Systems*, Beijing, China, pp.1-6, 2011.
[22] C. Xia, X. Na, X. Chai and T. Song, Analysis on mechanism and suppression of mechanical resonance in servo system, *Navigation Positioning and Timing*, vol.3, no.1, pp.29-35, 2016.

Author Biography

Chenyang Zhou received the B.S. degree in Electrical Engineering and Its Automation from Jiangsu Ocean University, Lianyungang, China, in 2011, and he received the Ph.D. degree in Control Science and Engineering from Jiangnan University, Wuxi, China. He joined the School of Electronic Engineering, Jiangsu Ocean University at 2023. He is currently working on Research on Resonance and Suppression of Drive Chain with Transmission Clearance in Wind Power System. His research interests include mechanical resonance suppression on wind power system.

Yanxia Shen received the Ph.D. degree in Power Electronics and Power Transmission from China University of Mining and Technology, Xuzhou, China in 2004, and she went to the Power Electronics Laboratory of University of California, Irvine for one year's visiting research in September 2007. She is currently a professor and doctoral supervisor at School of Internet of Things Engineering, Jiangnan University. Currently, she is a member of Jiangsu Power Electronics and Power Transmission Professional Committee, director of Jiangsu Electrical Engineering Society, deputy secretary general of Wuxi Automation Society, and a long-term reviewer of *Journal of Electric Machines and Control* and *IEEE Transactions on Power Electronics*. She is mainly engaged in the research of power electronics and power transmission technology, new energy technology and teaching of motion control system. She has published more than 60 academic papers in professional journals, among which more than 30 papers are indexed by SCI/EI. She has presided over or participated in 3 National Natural Science Foundation projects and 6 provincial and ministerial key projects. She has won 1 first prize and 1 second prize of provincial and ministerial science and technology progress award. In 2009, she was selected into the Excellent Talents Support Program of the Ministry of Education, and won many honorary titles such as Jiangsu Qingan Project Backstop Teacher and Wuxi Youth Science and Technology Award.

Yuanshen Zhou received the Ph.D. degree in Power Electronics and Power Transmission from China University of Mining and Technology, Xuzhou, China in 2004. He is the senior member of China Institute of Electrical Technology, member of China Institute of Electrical Engineering. He is now a professor at the School of Electronic Engineering, Jiangsu Ocean University, and his research field is power electronics technology and motor control, wind power system. Now he is a member of Jiangsu Provincial Association of Automation and a member of the Power Electronics and Power Transmission Committee of Jiangsu Provincial Institute of Electrical Technology. He is currently an evaluation expert of Graduate Degree Center of the Ministry of Education, and has long been a reviewer of *Journal of System Simulation*, *The Journal of Chinese Society for System Simulation*, and *Journal of Electric Machines and Control*, EI journal. More than 50 professional academic papers have been published. He has undertaken 2 projects of National Natural Science Foundation of China.